Finite Element Formulation for Thermal Buckling of Rails

David H. Allen
Gary D. Fry

Center for Railway Research
Texas A&M Transportation Institute
Texas A&M University System

CRR Report No. 2016-02
September 1, 2016

Center for Railway Research

Finite Element Formulation for Thermal Buckling of Rails

By
David H. Allen
Gary D. Fry

Abstract

A model is developed herein for predicting the onset of thermally induced buckling in the horizontal plane for rail structures. As described below, the model may be considered to be an extension of previous efforts spanning most of the twentieth century. Building on both previous analytic and computational solutions, a finite element model is developed for the purpose of predicting the thermal buckling temperature as a function of the track and support structure material properties, the track and support system geometries, the applied track loading, and the initial lateral displacement within the track. Particular emphasis is placed on nonlinearity and history dependence of the lateral track resistance to deformation. The resulting model is deployed herein to solve problems demonstrating usefulness of the model.

Introduction

Rails are known to undergo a variety of failure mechanisms that can cause significant property damage and loss of life (FRA 2015). It is therefore propitious to develop advanced models for the purpose of mitigating such mishaps. Toward this end, a one such model is presented herein.

The literature on this subject is long and deep. Historically, Galileo introduced the problem of a beam in bending in 1637 (Galileo 1637). More than a century later, the first cogent model for beam bending was reported by Euler and Bernoulli (Euler 1744). In the early twentieth century this approach was used to model the structural response of rails (Timoshenko 1915, 1927). Over the most recent half century a rigorous beam formulation of the rail thermal buckling problem has emerged (Kerr 1974, 1978). In addition, methods have been reported for solving the problem numerically (Tvergaard and Needleman 1981, Lim et al 2003).

Model Development

Consider a generic rail mounted on a railway, as shown in Fig. 1. Note that the x coordinate is aligned in the direction of travel, and the y and z coordinate axes are aligned with the vertical and horizontal directions, respectively.

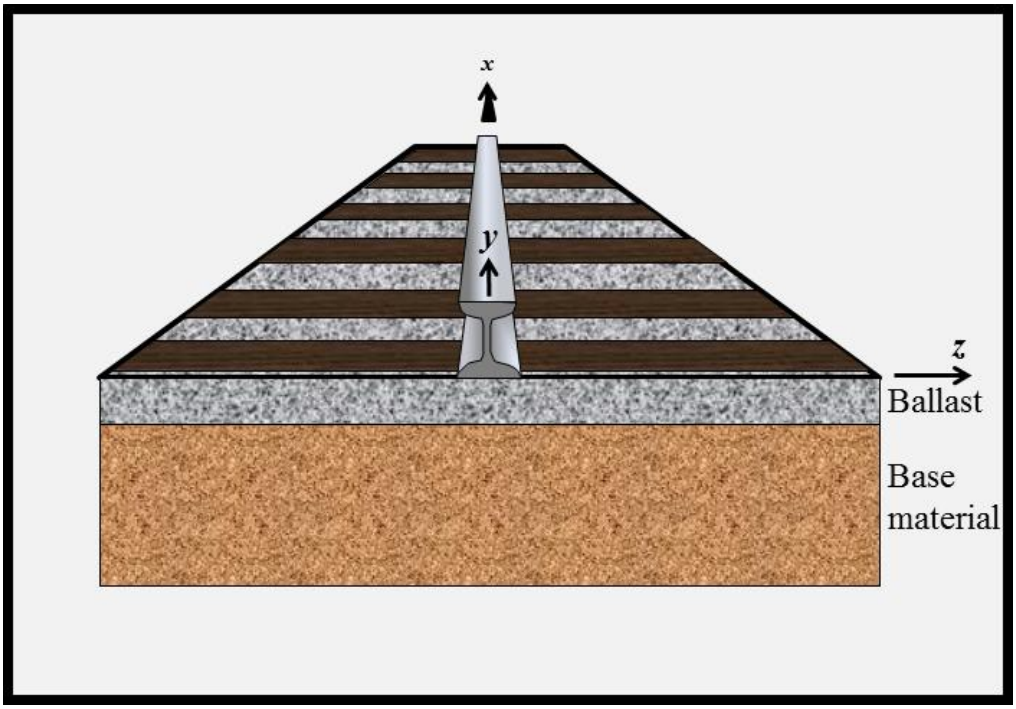

Fig. 1 Generic Rail with Coordinate Axes as Shown

When viewed from the bottom, a typical rail with mechanical and thermal loading is shown in Fig. 2.

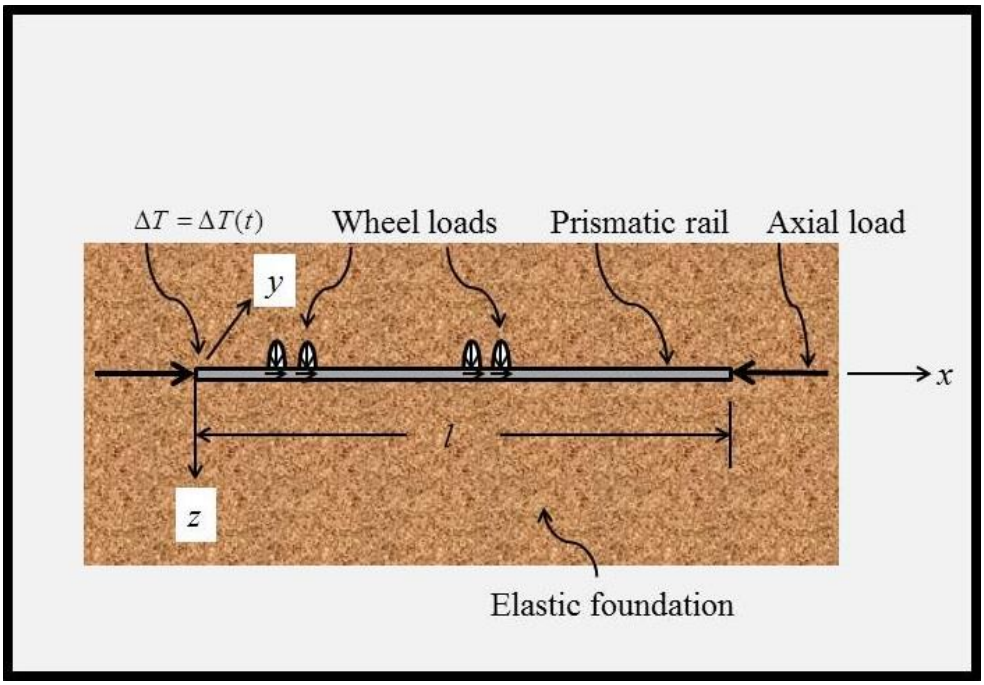

Fig. 2 Bottom View of Typical Rail Loaded Mechanically and Thermally

In order to construct a model of the rail, it is first assumed that it may be modeled as a beam-column, implying that it is long and slender (Allen and Haisler 1985). As shown in Fig. 3, the centroidal axis of the rail may deform in all three coordinate directions, and the components of this displacement are denoted by $u_0(x,t)$, $v_0(x,t)$ and $w_0 = w_0(x,t)$, respectively. Similarly, the components of stress are shown on an arbitrary cross-section of the rail in Fig. 4.

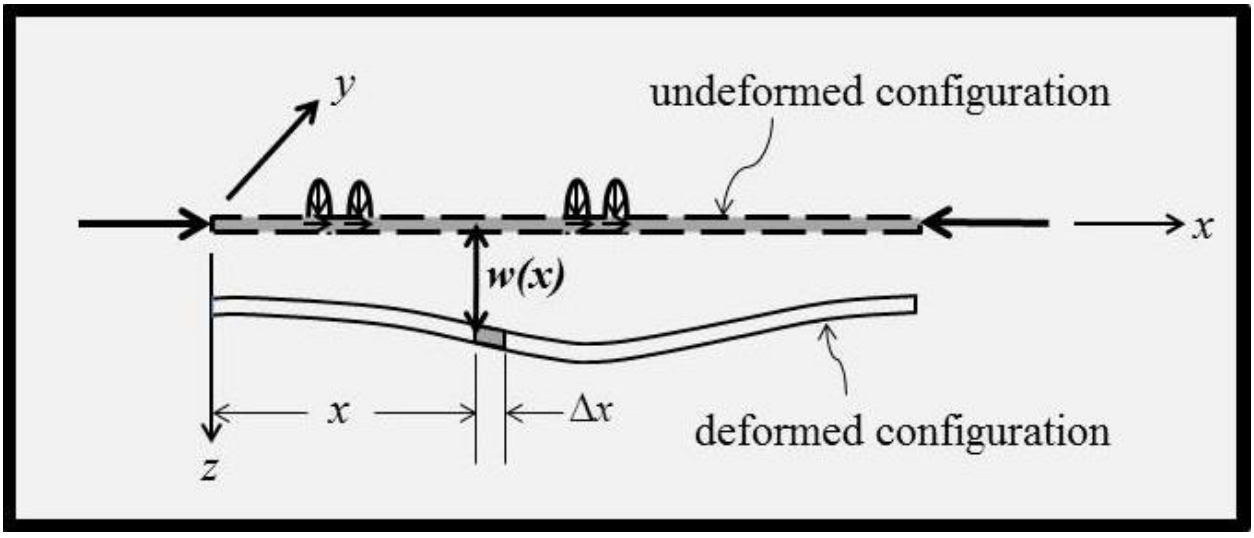

Fig. 3 Bottom View of the Rail Showing Horizontal Tranvserse Displacement Component in the Deformed Configuration

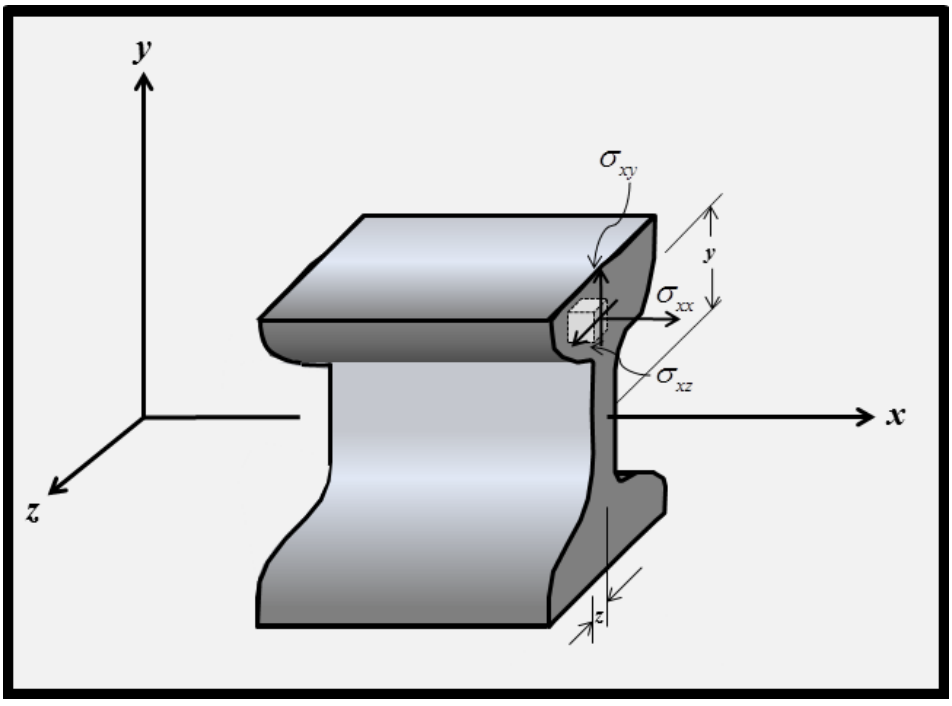

Fig. 4 Components of Stress on an Arbitrary Cross-Section of the Rail

A bottom view of a free body diagram of a section of the rail is constructed in Fig. 5, wherein the load per unit length applied to the centroidal axis of the rail is composed of components $p_x(x,t)$ and $p_z(x,t)$ in the *x* and *z* coordinate directions, respectively. In addition, the normal component of force per unit length applied to the bottom of the rail due to the normal displacement component $w(x,t)$ is denoted as $-k_z w(x,t)$, where the negative sign is employed so that the base stiffness is non-negative when the resultant is positive due to downward displacement of the rail. Similarly, the axial component of force per unit length applied to the bottom of the rail due to the axial component of displacement $u(x,t)$ is denoted as $-k_x u(x,t)$.

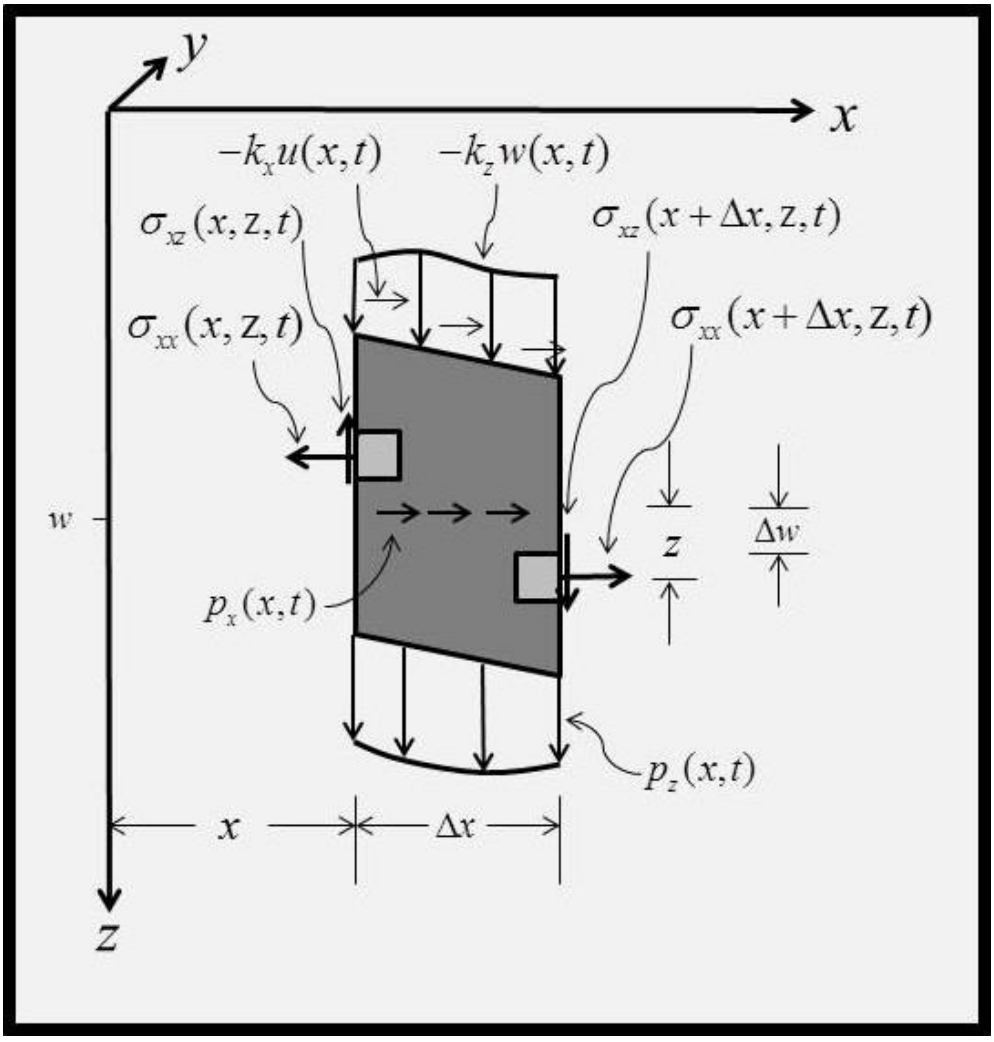

Fig. 5 Bottom View of Free Body Diagram of Cut Rail

Note also that the stress distribution on the two vertical cuts within the rail are denoted generically by the two infinitesimal stress boxes on these faces. Finally, note that the differential element is depicted in the deformed configuration, so that the axial force affects the transverse displacement of the rail. This necessarily causes the response of the rail to be geometrically nonlinear.

Consistent with Euler-Bernoulli beam theory the force and moment resultants are now defined as follows (Allen and Haisler 1985):

$$P = P(x,t) \equiv \int_A \sigma_{xx} dA \tag{1}$$

$$V_z = V_z(x,t) \equiv \int_A \sigma_{xz} dA \tag{2}$$

$$M_y = M_y(x,t) \equiv \int_A \sigma_{xx} z dA \tag{3}$$

where A is the cross-sectional area of the rail, and z is the horizontal distance from the centroid. The above resultants may now be utilized to construct the alternate free body diagram shown in Fig. 6.

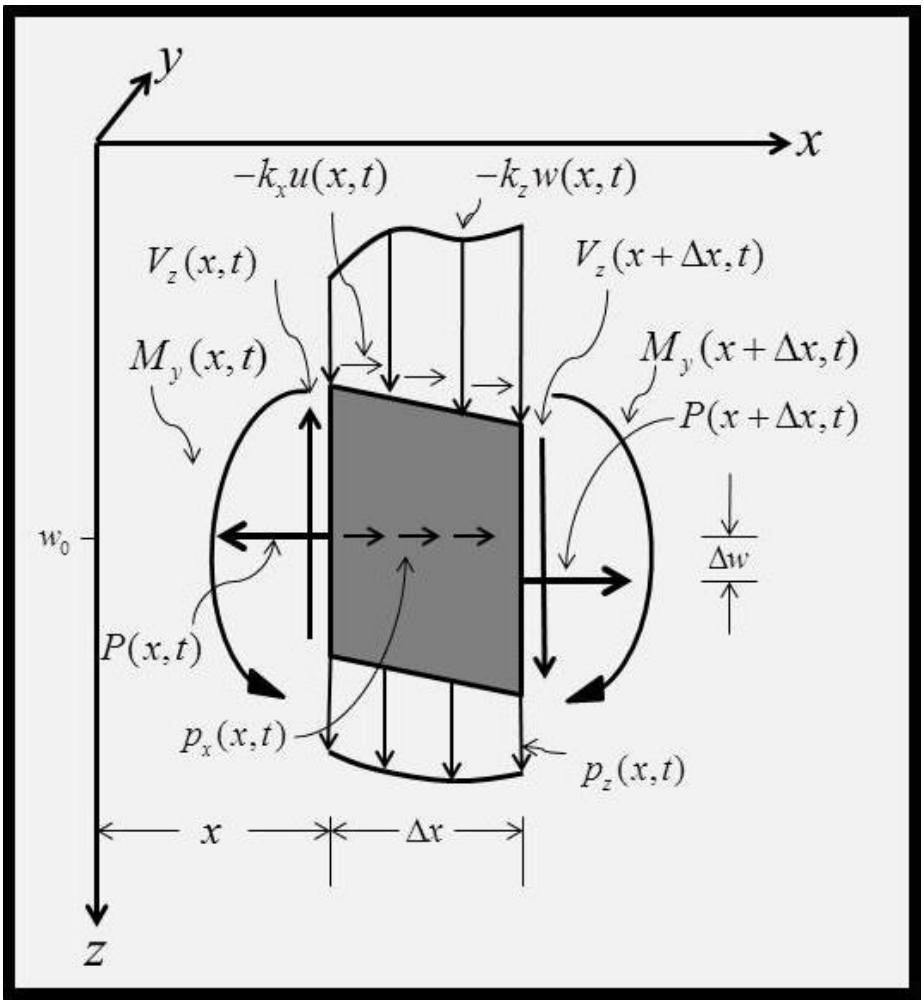

Fig. 6 Resultant Forces and Moments Applied to a Differential Element of the Rail

Employing the Euler-Bernoulli assumption (Euler 1744), assuming linear elastic behavior, and applying Newton's first law to the forces in the x coordinate direction in Fig. 6 will result in the general two dimensional formulation shown in Table 1 for a generic rail subjected to mechanical and thermal loading (Kerr 1974, 1978, Allen and Haisler 1985, Grissom and Kerr 2006).

Independent Variables: x,t

Known Inputs:

Loads: $p_x = p_x(x,t), p_z = p_z(x,t), \quad 0 < x < l$

Temperature change: $\Delta T = \Delta T(t) = known$

Geometry: l, h, A, I_{yy}

Material Properties: $\rho, \alpha, E, k_x, k_z$

Unknowns: $u, w, \sigma_{xx}, P, V_z, M_y$ = **6 unknowns**

Field Equations:

		No. of Equations
(A1)	$\frac{dP}{dx} = -p_x + k_x u$	1
(A2)	$\frac{dV_z}{dx} = k_z w - p_z$	1
(A3)	$\frac{dM_y}{dx} = V_z + P\frac{dw}{dx}$	1
(A4)	$\sigma_{xx} = \frac{(P + P^T)}{A} + \frac{M_y}{I_{yy}} z - E\alpha\Delta T$	1
(A5)	$\frac{\partial u}{\partial x} = \frac{(P + P^T)}{EA}$	1
(A6)	$\frac{\partial^2 w}{\partial x^2} = -\frac{M_y}{EI_{yy}}$	1
	Total	**6**

Table 1 Model for Predicting the Rail Response

It should be noted that the problem formulated in Table 1 may be exceedingly difficult to solve, depending on the loading conditions and the material properties involved. In the following section this problem will be simplified as much as is practical for the case of thermally induced lateral buckling

A. Governing Equations for Lateral Thermal Buckling

For the case of thermally induced lateral buckling, the following simplifying assumptions are made:

- The axial component of displacement in the rail structure is negligible
- The horizontal component of the displacement vector is independent of the vertical component of displacement
- Friction and externally applied loads in the axial direction may be neglected

Given these assumptions, equations (A1)-(A6) reduce to the following six governing equations:

$$\frac{dV_z}{dx} = k_z w - p_z \tag{4}$$

$$\frac{dM_y}{dx} = V_z - P^T \frac{dw}{dx} \tag{5}$$

$$\sigma_{xx} = \frac{P^T}{A} + \frac{M_y}{I_{yy}} z - E\alpha\Delta T \tag{6}$$

$$P^T = EA\alpha\Delta T \tag{7}$$

$$M_y = -EI_{yy} \frac{d^2 w}{dx^2} \tag{8}$$

where

x is the longitudinal dimension of the rail structure

z is the horizontal dimension of the rail structure

u is the rail structure displacement of the centroidal axis in the x coordinate direction

w is the rail structure displacement of the centroidal axis in the z coordinate direction

P^T is the thermally induced axial force resultant in the x coordinate direction

V_z is the lateral force resultant in the z coordinate direction

M_y is the resultant moment about the z coordinate axis

p_z is the externally applied load per unit length in the z coordinate direction

σ_{xx} is the normal stress component in the x direction

A is the cross-sectional area of the rail structure

I_{yy} is the moment of inertia about the y axis

E is Young's modulus of the rail

α is the coefficient of thermal expansion of the rail

ΔT is the temperature change from the rail neutral temperature

In the above formulation x is the independent variable, and the following are assumed to be known inputs:

Loads: $p_z = 0$

Temperature change: ΔT

Geometry: l, h, A, I_{yy}

Material Properties: ρ, α, E, k_z

Therefore, when proper boundary conditions are constructed, the above represents six equations in the following six dependent variables: $w, \sigma_{xx}, P^T, V_z, M_y$.

B. Variational Formulation

In order to construct a finite element algorithm for solving the above problem it is first necessary to construct a variational principle for describing the problem. In order to do this, first reduce the shear term out of the problem by rearranging equation (5) and substituting this result into equation (4), thereby resulting in the following equation:

$$\frac{\partial}{\partial x}\left(\frac{\partial M_y}{\partial x} + P^T \frac{\partial w}{\partial x}\right) = k_z w - p_z \tag{9}$$

A variation form of equations (12) and (15) may now be constructed by integrating these two equations against variations in their energy conjugates and adding them together, thereby resulting in the following variational principle:

$$\int_0^l \left[\frac{d}{dx}\left(\frac{dM_y}{dx} + P^T \frac{dw}{dx}\right) - k_z w + p_z\right]\delta w dx = 0 \tag{10}$$

where l is an arbitrary longitudinal dimension over which the integration is to be performed, and $\theta = dw/dx$ is the rotation about the y axis. Now, integrating the differentiated terms by parts results in the following:

$$\begin{aligned} &-\int_0^l \left(\frac{dM_y}{dx} + P^T \frac{dw}{dx}\right)\delta\left(\frac{dw}{dx}\right)dx \\ &\quad -\int_0^l k_z w \delta w dx + \int_0^l p_z \delta w dx + \left(\frac{dM_y}{dx} - P^T \frac{dw}{dx}\right)\delta w\Big|_0^l = 0 \end{aligned} \tag{11}$$

Substituting equations (5) and (8) into equation (11) now results in the following:

$$-\int_0^l \frac{d}{dx}\left(-EI_{yy}\frac{d^2w}{dx^2}\right)\delta\left(\frac{dw}{dx}\right)dx-\int_0^l P^T\frac{dw}{dx}\delta\left(\frac{dw}{dx}\right)dx$$
$$-\int_0^l k_z w\delta w dx+\int_0^l p_z\delta w dx+V_z\delta w\Big|_0^l=0 \tag{12}$$

Now, integrating the higher order term in equation (12) by parts one more time results in the following variation principle:

$$\int_0^l EI_{yy}\frac{d^2w}{dx^2}\delta\frac{d^2w}{dx^2}dx+\int_0^l P^T\frac{dw}{dx}\delta\left(\frac{dw}{dx}\right)dx+\int_0^l k_z w\delta w dx$$
$$=\int_0^l p_z\delta w dx+V_z\delta w\Big|_0^l+M_y\,\delta\theta\Big|_0^l \tag{13}$$

The above is the final form of the variational principle to be implemented within the finite element method.

C. Finite Element Formulation

Equation (13) may now be discretized for a generic frame element. To do this, it is assumed that, within a generic element of length, l_e, the displacement field may be approximated by the following (Reddy 1984, Allen and Haisler 1985):

$$w^e=c_3+c_4\bar{x}+c_5\bar{x}^2+c_6\bar{x}^3 \tag{14}$$

Satisfying boundary conditions at the end points of the local element will result in the following from of equation (14) (Reddy 1984):

$$w^e=\phi_1^e w_1^e+\phi_2^e\theta_1^e+\phi_3^e w_2^e+\phi_4^e\theta_2^e \tag{15}$$

where w_1^e and w_2^e are the lateral displacement components at the left and right ends of element *e*, and θ_1^e and θ_2^e are the rotation components about the y-axis at the left and right ends of element *e*. The shape functions are given by:

$$
\begin{aligned}
\phi_1^e &= 1-3\left(\frac{\overline{x}}{l_e}\right)^2+2\left(\frac{\overline{x}}{l_e}\right)^3 \\
\phi_2^e &= \overline{x}\left(1-\frac{\overline{x}}{l_e}\right)^2 \\
\phi_3^e &= 3\left(\frac{\overline{x}}{l_e}\right)^2-2\left(\frac{\overline{x}}{l_e}\right)^3 \\
\phi_4^e &= \overline{x}\left[\left(\frac{\overline{x}}{l_e}\right)^2-\frac{\overline{x}}{l_e}\right]
\end{aligned}
\tag{16}
$$

The assumed displacement field within a generic element represented by equations (13) and (15) may now be substituted into variational principle (13), thereby resulting in algebraic equations of the following form for a generic element (Reddy 1984, Allen and Haisler 1985):

$$
\sum_{j=1}^{6} K_{ij}^e q_j^e + \sum_{j=1}^{6} B_{ij}^e q_j^e + \sum_{j=1}^{6} N_{ij}^e q_j^e = F_i^e \qquad i = 1,...,6 \tag{17}
$$

where the second term above accounts for the second term in equation (13), and the third term above accounts for the third term in equation (13). In addition,

$$
\left\{q^e\right\} \equiv \begin{Bmatrix} u_1^e \\ w_1^e \\ \theta_1^e \\ u_2^e \\ w_2^e \\ \theta_2^e \end{Bmatrix} \tag{18}
$$

and

$$\left[K^e\right]=\begin{bmatrix} \frac{E^eA^e}{l^e} & 0 & 0 & -\frac{E^eA^e}{l^e} & 0 & 0 \\ 0 & \frac{12E^eI^e_{yy}}{(l^e)^3} & \frac{6E^eI^e_{yy}}{(l^e)^2} & 0 & -\frac{12E^eI^e_{yy}}{(l^e)^3} & \frac{6E^eI^e_{yy}}{(l^e)^2} \\ 0 & \frac{6E^eI^e_{yy}}{(l^e)^2} & \frac{4E^eI^e_{yy}}{l^e} & 0 & -\frac{6E^eI^e_{yy}}{(l^e)^2} & \frac{2E^eI^e_{yy}}{l^e} \\ -\frac{E^eA^e}{l^e} & 0 & 0 & \frac{E^eA^e}{l^e} & 0 & 0 \\ 0 & -\frac{12E^eI^e_{yy}}{(l^e)^3} & -\frac{6E^eI^e_{yy}}{(l^e)^2} & 0 & \frac{12E^eI^e_{yy}}{(l^e)^3} & -\frac{6E^eI^e_{yy}}{(l^e)^2} \\ 0 & \frac{6E^eI^e_{yy}}{(l^e)^2} & \frac{2E^eI^e_{yy}}{l^e} & 0 & -\frac{6E^eI^e_{yy}}{(l^e)^2} & \frac{4E^eI^e_{yy}}{l^e} \end{bmatrix} \tag{19}$$

Furthermore, for a linearly varying distributed lateral load given by

$$p_z(\bar{x}) = p_z^0 + (p_z^{l^e} - p_z^0)\frac{\bar{x}}{l^e} \tag{20}$$

$$\left\{F^e\right\}=\begin{Bmatrix} \frac{p_x l^e}{2} - E^eA^e\alpha^e\Delta T^e \\ \frac{p_z^0 l^e}{2} + \frac{3l^e}{20}\left(p_z^{l^e} - p_z^0\right) \\ \frac{p_z^0(l^e)^2}{12} + \frac{(l^e)^2}{30}\left(p_z^{l^e} - p_z^0\right) \\ \frac{p_x l^e}{2} + E^eA^e\alpha^e\Delta T^e \\ \frac{p_z^0 l^e}{2} + \frac{7l^e}{20}\left(p_z^{l^e} - p_z^0\right) \\ -\frac{p_z^0(l^e)^2}{12} - \frac{(l^e)^2}{20}\left(p_z^{l^e} - p_z^0\right) \end{Bmatrix} \tag{21}$$

Note that the boundary terms are not included because they will cancel one another when the global equations are assembled.

When the second and third terms may be neglected in equation (17), the standard finite element formulation for a linear thermoelastic beam undergoing small displacements is recovered. However, in the current case it remains to account for the second and third terms in equation (17).

Consider first the second term in equation (17). This term is given by

$$\left\{B^e\right\} = P^T \begin{bmatrix} 0 & 0 & 0 & 0 & 0 & 0 \\ 0 & \frac{6}{5l^e} & 0.10 & 0 & -\frac{6}{5l^e} & 0.10 \\ 0 & 0.10 & \frac{2l^e}{15} & 0 & -0.10 & -\frac{l^e}{30} \\ 0 & 0 & 0 & 0 & 0 & 0 \\ 0 & -\frac{6}{5l^e} & -0.10 & 0 & \frac{6}{5l^e} & -0.10 \\ 0 & 0.10 & -\frac{l^e}{30} & 0 & -0.10 & \frac{2l^e}{15} \end{bmatrix} \tag{22}$$

Now consider the third term in equation (17). In the case wherein it is sufficiently accurate to assume that the coefficient of friction, k_z, is constant in each element, these are as follows:

$$\left[N^e\right] = k_z \begin{bmatrix} 0 & 0 & 0 & 0 & 0 & 0 \\ 0 & \frac{13l_e}{35} & \frac{11(l_e)^2}{210} & 0 & \frac{9l_e}{70} & \frac{-78(l_e)^2}{2520} \\ 0 & \frac{11(l_e)^2}{210} & \frac{(l_e)^3}{105} & 0 & \frac{13(l_e)^2}{420} & -\frac{13(l_e)^3}{140} \\ 0 & 0 & 0 & 0 & 0 & 0 \\ 0 & \frac{9l_e}{70} & \frac{13(l_e)^2}{420} & 0 & \frac{13l_e}{35} & \frac{-11(l_e)^2}{210} \\ 0 & \frac{-78(l_e)^2}{2520} & -\frac{13(l_e)^3}{140} & 0 & \frac{-11(l_e)^2}{210} & \frac{(l_e)^3}{105} \end{bmatrix} \tag{23}$$

The above element equations may be assembled into a global finite element formulation using the standard assembly technique, and this has been accomplished by the authors. This then completes the finite element formulation for the case wherein the friction coefficient, k_z, is temporally constant. The following section will present several example problems for the purpose of validating the linear finite element algorithm developed herein.

D. Validation Problems for the Linear Case

The finite element algorithm is now validated for the linear case ($k_z = k_z^0 =$ constant) with the following example problems.

Example Problem #1

Given: A double-cantilevered beam is subjected to an evenly distributed loading $p_z = p_z^0 = 10^4\, N/m$. In addition, E=2.06x10^{11} N/m^2, I_{yy}=8.99x10^{-6} m^4, and l=12 m.

Required: **a)** Solve for $w = w(x, p_z^0, E, I_{yy})$ analytically

b) Obtain a solution for $w = w(x, p_z^0, E, I_{yy})$ numerically and compare the two solutions

Solution: a) For this case ($\Delta T = k_z = 0$) equation (15) simplifies to the following:

$$\frac{d^2}{dx^2}\left(EI_{yy}\frac{d^2w}{dx^2}\right) = p_z^0 \tag{E1.1}$$

Now integrate equation (E1.1) to obtain:

$$\frac{d}{dx}\left(EI_{yy}\frac{d^2w}{dx^2}\right) = p_z^0 x + c_1 \tag{E1.2}$$

where c_1 is a constant of integration. Integrating a second time gives:

$$EI_{yy}\frac{d^2w}{dx^2} = p_z^0\frac{x^2}{2} + c_1 x + c_2 \tag{E1.3}$$

where c_2 is a constant of integration. Integrating a third time gives:

$$\frac{dw}{dx} = \frac{1}{EI_{yy}}\left[p_z^0\frac{x^3}{6} + c_1\frac{x^2}{2} + c_2 x + c_3\right] \tag{E1.4}$$

where c_3 is a constant of integration. Integrating a fourth time gives:

$$w = \frac{1}{EI_{yy}}\left[p_z^0\frac{x^4}{24} + c_1\frac{x^3}{6} + c_2\frac{x^2}{2} + c_3 x + c_4\right] \tag{E1.5}$$

Next apply the following boundary condition:

$$w(x=0) = 0 \Rightarrow c_4 = 0 \tag{E1.6}$$

Next apply the following boundary condition:

$$\frac{dw}{dx}(x=0)=0 \Rightarrow c_3=0 \tag{E1.7}$$

Substituting equations (E1.6) and (E1.7) into equation (E1.5) results in the following:

$$w=\frac{1}{EI_{yy}}\left[p_z^0\frac{x^4}{24}+c_1\frac{x^3}{6}+c_2\frac{x^2}{2}\right] \tag{E1.8}$$

Next apply the following boundary condition:

$$w(x=l)=0 \Rightarrow 0=p_z^0\frac{l^4}{24}+c_1\frac{l^3}{6}+c_2\frac{l^2}{2} \tag{E1.9}$$

Now apply the final boundary condition:

$$\frac{dw}{dx}(x=l)=0 \Rightarrow 0=p_z^0\frac{l^3}{6}+c_1\frac{l^2}{2}+c_2 l \tag{E1.10}$$

Equations (E1.9) and (E1.10) are two equations in the two unknown coefficients c_1 and c_2 . Solving for these two unknowns results in the following:

$$c_1=-p_z^0\frac{l}{2} \qquad c_2=p_z^0\frac{l^2}{12} \tag{E1.11}$$

Substituting (E1.11) into (E1.8) therefore results in the following exact solution:

$$w=\frac{p_z^0}{EI_{yy}}\left[\frac{x^4}{24}-\frac{l}{12}x^3+\frac{l^2}{24}x^2\right] \tag{E1.12}$$

In addition, substituting (E6) and (E10) into (E3) results in:

$$\frac{dw}{dx}=\frac{p_z^0}{EI_{yy}}\left[\frac{x^3}{6}-\frac{l}{4}x^2+\frac{l^2}{12}x\right] \tag{E1.13}$$

b) The finite element algorithm is now deployed using 6 elements of equal length. Comparative results are shown in Fig. 7.

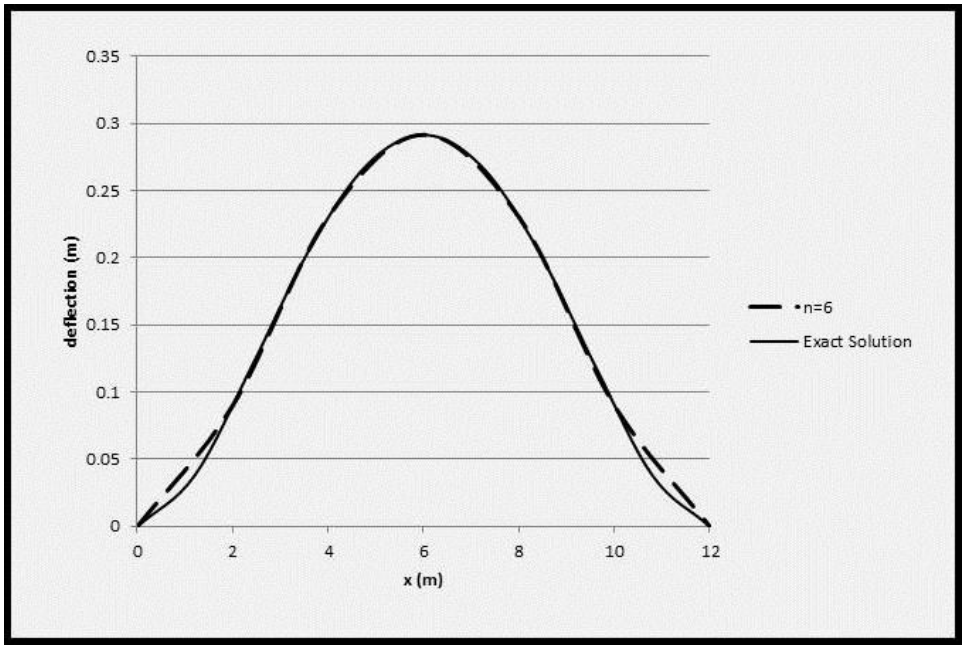

Fig. 7 Comparison of Computational Result to Exact Solution for Example Problem #1

Example Problem #2

Given: A cantilevered beam is subjected to the triangular distributed loading shown below with $p_z = p_z^0 = 10^4\, N/m$. In addition, E=2.06x10^{11} N/m^2, I_{yy}=8.99x10^{-6} m^4, and l=12 m.

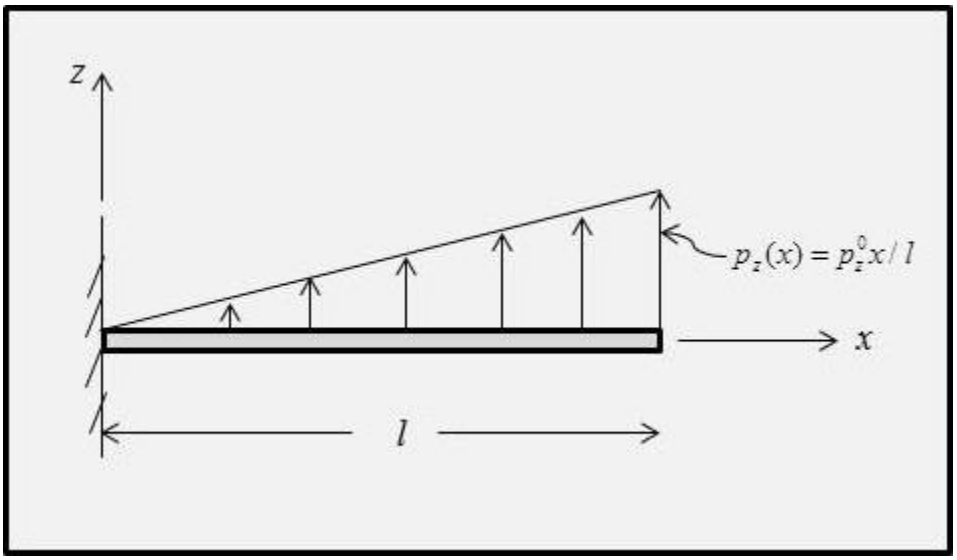

Fig. 8 Depiction of a Prismatic Cantilever Beam Subjected to Triangular Loading

Required: **a)** Solve for $w = w(x, p_z^0, E, I_{yy})$ analytically

b) Obtain a solution for $w = w(x, p_z^0, E, I_{yy})$ numerically and compare the two solutions

a) To obtain the analytic solution to this problem, first note that

$$p_z(x) = p_z^l \frac{x}{l} \tag{E2.1}$$

Now recall that the beam shear, $V_z(x)$, is given by the following:

$$\frac{dV_z}{dx} = -p_z \tag{E2.2}$$

Therefore, substituting (1) into (2) and integrating results in the following:

$$\int \frac{dV_z}{dx} dx = -\int p_z^l \frac{x}{l} dx \Rightarrow V_z(x) = -p_z^l \frac{x^2}{2l} + c_1 \tag{E2.3}$$

Now consider the following boundary condition:

$$V_z(x = l) = 0 \tag{E2.4}$$

Substituting (4) into (3) gives the following:

$$c_1 = \frac{p_z^l l}{2} \Rightarrow V_z(x) = -\frac{p_z^l}{2l}\left(x^2 - l^2\right) \tag{E2.5}$$

Now recall the beam moment, $M_y(x)$, is given by the following:

$$\frac{dM_y}{dx} = V_z \tag{E2.6}$$

Therefore, substituting (5) into (6) results in the following:

$$\frac{dM_y}{dx} = -\frac{p_z^l}{2l}\left(x^2 - l^2\right) \tag{E2.7}$$

Integrating equation (7) therefore gives the following:

$$M_y(x) = -\frac{p_z^l}{2l}\left(\frac{x^3}{3} - l^2 x\right) + c_2 \tag{E2.8}$$

Now consider the following boundary condition:

$$M_y(x = l) = 0 \tag{E2.9}$$

Substituting (9) into (8) gives the following:

$$c_2 = \frac{p_z^l l^2}{3} \Rightarrow M_y(x) = -\frac{p_z^l}{2l}\left(\frac{x^3}{3} - l^2 x + \frac{2l^3}{3}\right) \tag{E2.10}$$

Now consider the following equation:

$$\frac{d^2 w}{dx^2} = -\frac{M_y}{EI_{yy}} \tag{E2.11}$$

Substituting (10) into (11) thus results in:

$$\frac{d^2w}{dx^2} = \frac{p_z^l}{2lEI_{yy}}\left(\frac{x^3}{3} - l^2x + \frac{2l^3}{3}\right) \tag{E2.12}$$

Integrating the above thus gives:

$$\theta_y(x) = \frac{dw}{dx} = \frac{p_z^l}{2lEI_{yy}}\left(\frac{x^4}{12} - \frac{l^2x^2}{2} + \frac{2l^3x}{3}\right) + c_3 \tag{E2.13}$$

Now consider the following boundary condition:

$$\theta_y(x=0) = 0 \tag{E2.14}$$

Substituting (14) into (13) gives the following:

$$c_3 = 0 \Rightarrow \theta_y(x) = \frac{p_z^l}{2lEI_{yy}}\left(\frac{x^4}{12} - \frac{l^2x^2}{2} + \frac{2l^3x}{3}\right) \tag{E2.15}$$

It follows that

$$\theta_y(x=l) = -\frac{1p_z^l l^3}{8EI_{yy}} \tag{E2.16}$$

Integrating equation (15) gives the following:

$$w(x) = \frac{p_z^l}{2lEI_{yy}}\left(\frac{x^5}{60} - \frac{l^2x^3}{6} + \frac{l^3x^2}{3}\right) + c_4 \tag{E2.17}$$

Now consider the following boundary condition:

$$w(x=0) = 0 \tag{E2.18}$$

Substituting (18) into (17) results in the following:

$$c_4 = 0 \Rightarrow w(x) = \frac{p_z^l}{2lEI_{yy}}\left(\frac{x^5}{60} - \frac{l^2x^3}{6} + \frac{l^3x^2}{3}\right) \tag{E2.19}$$

It follows that

$$w(x=0) = \frac{11p_z^l l^4}{120EI_{yy}} \tag{E2.20}$$

b) The finite element solution is obtained using 6 elements of equal length. Comparative results are shown in Fig. 9.

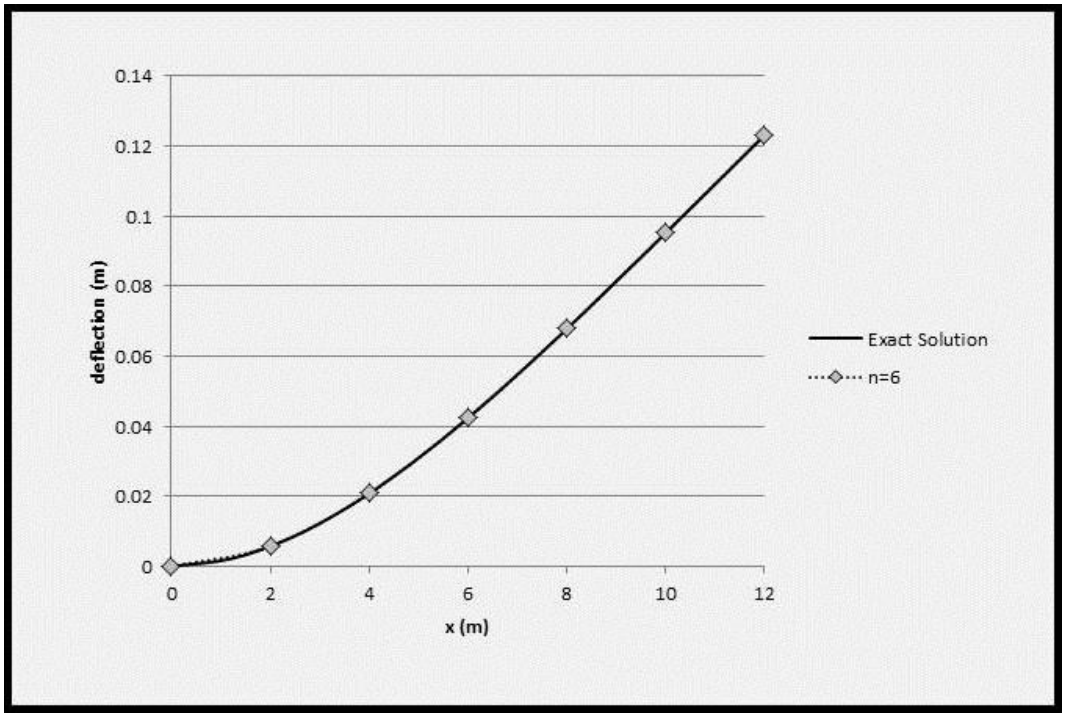

Fig. 9 Comparison of Computational Result to Exact Solution for Example Problem #2

Example Problem #3

Given: A simply beam is subjected to a temperature change of $\Delta T = 50\,°C$. Properties are E=2.06x10^{11} N/m^2, I_{yy}=8.99x10^{-6} m^4, $k_z = 10^5\ N/m^2$ A=0.0145 m^2, l=8.0 m and $\alpha = 1.05x10^{-5}/°C$.

Required: a) Obtain an analytic for $w = w(x, p_z^0, E, I_{yy})$.

b) obtain a solution using finite elements and compare the two

Solution: a) The solution solves the following differential equation:

$$EI_{yy}\frac{d^4w}{dx^4} - P^T\frac{d^2w}{dx^2} = p_z \tag{E3.1}$$

In order to obtain an analytic solution, assume that the solution is of the form:

$$w(x) = a_0 + a_1x + a_2x^2 + a_3x^3 + a_4x^4 \tag{E3.2}$$

Next, consider the boundary conditions:

$$\text{at x=0, } l\text{: } w = 0, \frac{d^2w}{dx^2} = 0 \tag{E3.3}$$

in order for (E3.2) to be a correct assumption, it must satisfy both (E3.1) and (E3.3). First, satisfy (E(3.3) as follows:

$$\frac{d^2w}{dx^2} = \frac{d}{dx^2}\left(a_0 + a_1x + a_2x^2 + a_3x^3 + a_4x^4\right) = 2a_2 + 6a_3x + 12a_4x^2 \tag{E3.4}$$

Satisfying (E3.3) with (E3.4) results in the following:

$$a_2 = 0, a_4 = -\frac{a_3}{2l} \tag{E3.5}$$

Substituting (E3.5) into (E3.2) gives the following:

$$w(x) = a_0 + a_1x + a_3x^3 - \frac{a_3}{2l}x^4 \tag{E3.6}$$

Satisfying (E3.3) gives the following for (E3.6)

$$a_0 = 0, a_1 = -\frac{a_3l^2}{2} \tag{E3.7}$$

Substituting (E3.7) into (E3.6) gives:

$$w(x) = a_3\left(-\frac{l^2x}{2} + x^3 - \frac{x^4}{2l}\right) \tag{E3.8}$$

Substituting (E3.8) into (E3.2) results in the following:

$$\begin{aligned} EI_{yy}\frac{d^4}{dx^4}\left[a_3\left(-\frac{l^2x}{2} + x^3 - \frac{x^4}{2l}\right)\right] - P^T\frac{d^2}{dx^2}\left[a_3\left(-\frac{l^2x}{2} + x^3 - \frac{x^4}{2l}\right)\right] = p_z \Rightarrow \\ p_z = -\frac{12a_3EI_{yy}}{l} - P^Ta_3\left(+6x - 6\frac{x^2}{l}\right) \end{aligned} \tag{E3.9}$$

Thus, the distributed loading given by (E3.9) provides the exact solution given by (E3.8).

b) The finite element solution for several different numbers of elements is compared to the exact solution in Fig. 10, wherein it can be seen that convergence is obtained with twelve elements of equal length.

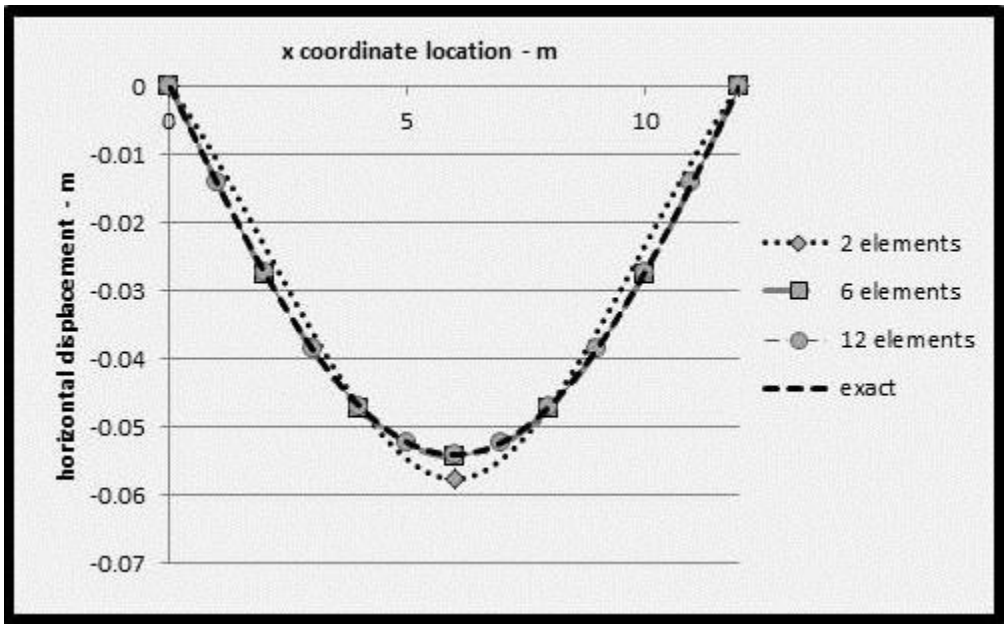

Fig. 10 Comparison of Computational Result to Exact Solution for Example Problem #3

Example Problem #4

Given: A double-cantilevered beam is subjected to a distributed loading, where E=2.06x10^{11} N/m^2, I_{yy}=8.99x10^{-6} m^4, $k_z = k_z^0 = 10^5\ N/m^2$ A=0.0145 m^2 and l=8.0 m. In addition, $\alpha = 1.05x10^{-5}/°C$ and $\Delta T = 50\,°C$.

Required: a) Obtain an analytic solution for $w = w(x, p_z^0, E, I_{yy})$.

b) obtain a solution using finite elements and compare the two

Solution: a) The solution solves the following differential equation:

$$EI_{yy}\frac{\partial^4 w}{\partial x^4} + P\frac{\partial^2 w}{\partial x^2} + k_z w = p_z \qquad \text{(E4.1)}$$

Suppose that we choose the following:

$$w(x) = C_1\left[x^2 - \frac{2x^3}{l} + \frac{x^4}{l^2}\right] \qquad 0 \le x \le l \qquad \text{(E4.2)}$$

where l is the length of the beam and C_1 is a loading constant. It can be seen that the above assumed solution satisfies the following boundary conditions:

$$w(x=0,l)=0$$
$$\frac{dw}{dx}(x=0,l)=0 \qquad \text{(E4.3)}$$

In order to obtain the forcing function, p_z, equation (E4.2) is now substituted into equation (E4.1) and it is solved, thereby resulting in the following:

$$p_z(x)=C_1EI_{yy}\frac{d^4}{dx^4}\left[x^2-\frac{2x^3}{l}+\frac{x^4}{l^2}\right]+C_1P\frac{d^2}{dx^2}\left[x^2-\frac{2x^3}{l}+\frac{x^4}{l^2}\right]+C_1k_z^0\left[x^2-\frac{2x^3}{l}+\frac{x^4}{l^2}\right]$$
$$=\frac{24C_1EI_{yy}}{l^2}+C_1P\left(2-\frac{12x}{l}+\frac{12x^2}{l^2}\right)+C_1k_z^0\left[x^2-\frac{2x^3}{l}+\frac{x^4}{l^2}\right] \qquad \text{(E4.4)}$$

Equation (E4.2) is then the solution for a double cantilever beam with constant coefficient of friction and constant temperature change given by equation (2) subjected to forcing function given by equation (E4.4) and with boundary conditions (E4.3).

c) The finite element solution gives the results shown in Fig. 11.

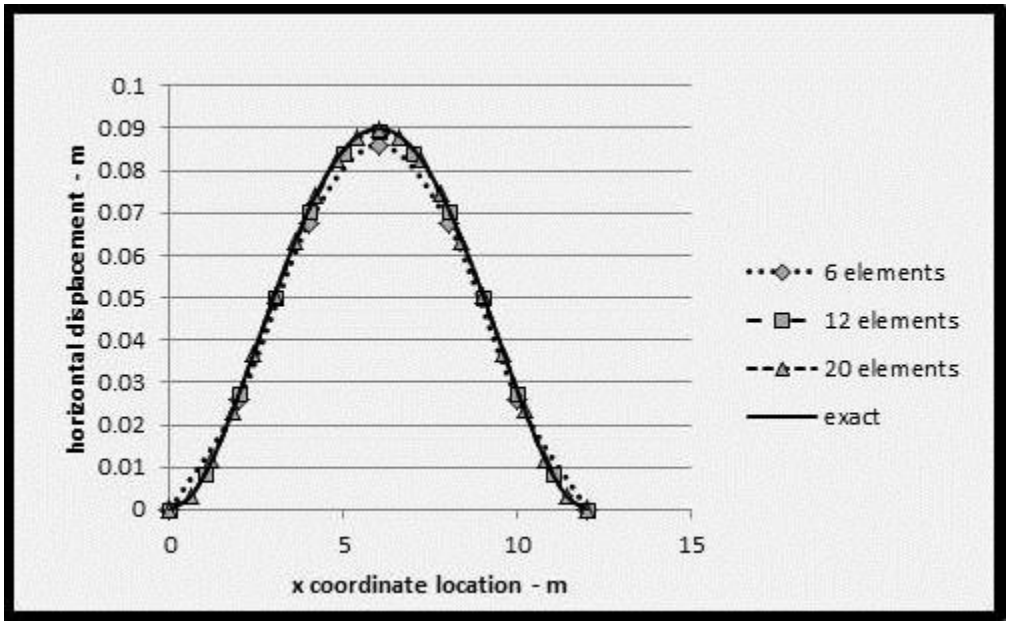

Fig. 11 Comparison of Computational Result to Exact Solution for Example Problem #4

It can be seen from the above example problems that the finite element model reproduces the exact solution for the linear case, with convergence obtained with 20 elements of equal length.

E. Modeling the Rail Response for the Nonlinear Case

Now consider the third term in equation (17) once again. This term will necessarily be nonlinear whenever the coefficient of friction, k_z, is not constant, and this circumstance is the main purpose of the current study. The nonlinearity enters via the dependence of the friction coefficient, k_z, on the lateral displacement, w. As shown in Fig. 12, single tie push tests (STPT) confirm this nonlinearity.

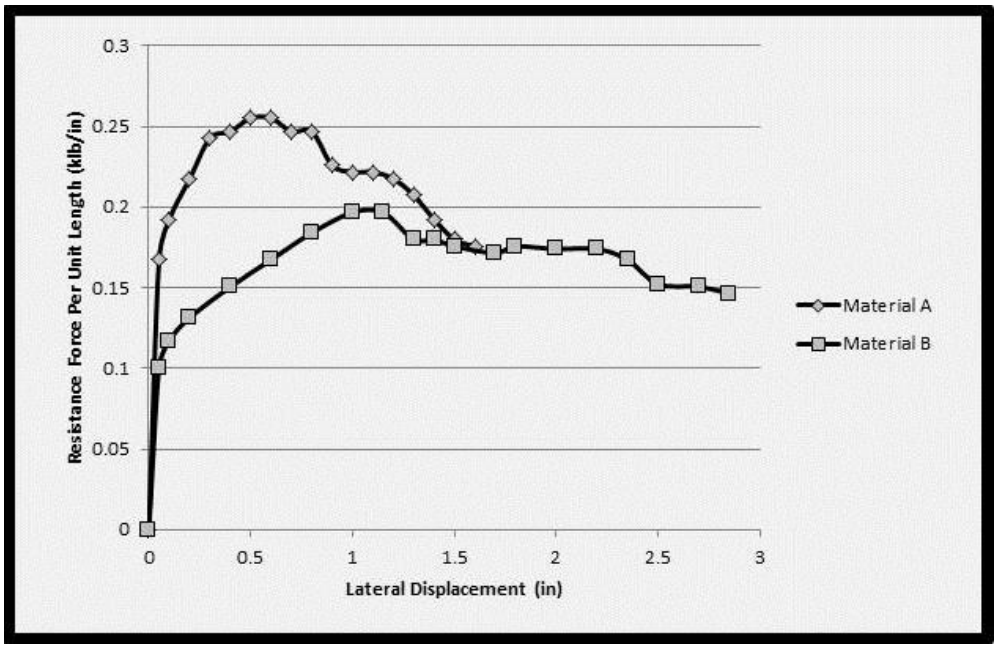

Fig. 12 Typical Lateral Load vs. Displacement from STPT Tests (Read et al 2011)

For a given rail structure configuration, the above response is typically modeled with a power law of the following form (Tvergaard and Needleman 1981, Allen et al. 2016):

$$k_z(w) = k_z^0 - k_z^1\left(\frac{w}{w_0}\right)^n \tag{24}$$

As shown in Fig. 13, this type of curve fit does an adequate job of predicting the observed nonlinearity in the coefficient of lateral friction.

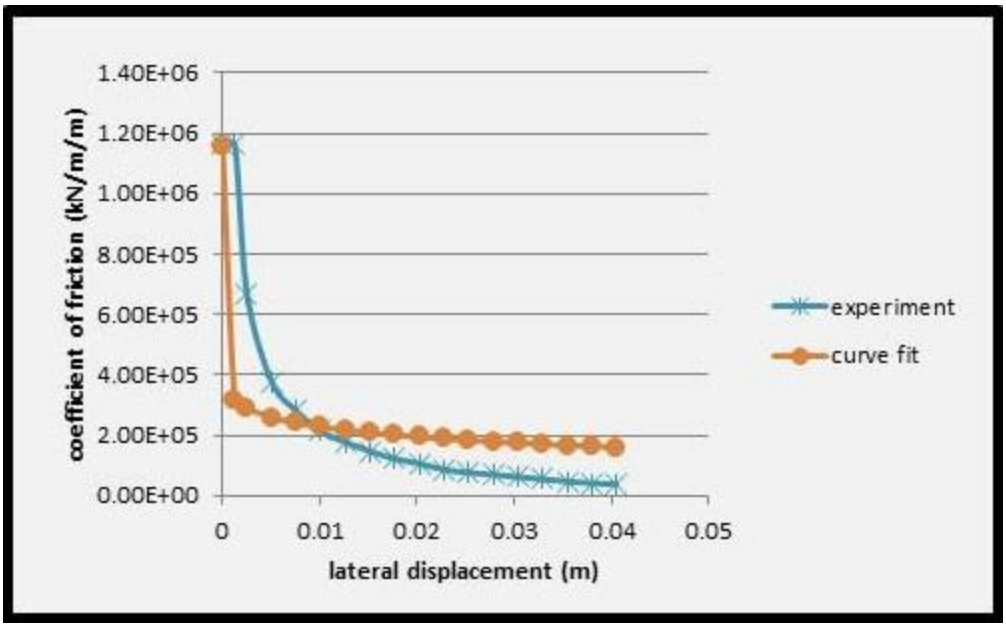

Fig. 13 Comparison of Predicted Coefficient of Lateral Friction to Experimental Data Using Equation (24)

As can be seen from Fig. 13, the coefficient of lateral friction can be highly nonlinear. Accordingly, failing to account for this nonlinearity in the model can lead to significant predictive error in the model. Therefore, it is essential to include the ability to predict this nonlinearity in the model. Toward this end, a standard time marching scheme is adopted herein, in which the externally applied mechanical load is gradually increased in a series of time steps, with Newton iteration deployed to capture the nonlinearity on each time step (Little et al. 2016).

Briefly, this is accomplished by first obtaining an approximate solution in which it is assumed that in the term k_z the displacement from the previous time step is used, thereby resulting in the following first approximation for the global form of equation (17).

$$\sum_{j=1}^{6} K_{ij}^{e} \Delta q_j^0 + \sum_{j=1}^{6} B_{ij}^{e} \Delta q_j^0 + \sum_{j=1}^{6} N_{ij}^{e} \Delta q_j^0 = \Delta F_i^e \tag{25}$$

This erroneous value of $\Delta w^m(x)$ can be utilized to reduce the error by employing Newton's method as follows:

$$\sum_{j=1}^{n} a_{ij} \Delta\Delta q_j^{m+1} = \Delta f_i(t+\Delta t), i = 1,...,n \tag{26}$$

where n is the number of spaces, and the coefficients a_{ij} are obtained by differentiating equation (25) with respect to the incremental nodal displacements, Δq_j, as follows [Ketter and Prawel 1969, Little et al. 2016]:

$$a_{ij} = \frac{\partial}{\partial \Delta q_j}\left(\sum_{j=1}^{6} K_{ij}^{e} \Delta q_j^0 + \sum_{j=1}^{6} B_{ij}^{e} \Delta q_j^0 + \sum_{j=1}^{6} N_{ij}^{e} \Delta q_j^0 \right) \tag{27}$$

In addition, the global force matrix on each iteration is given by the following (Little et al. 2016):

$$\Delta f_i(t+\Delta t) = \Delta F_i - \Delta R_i, i = 1,...,n \tag{28}$$

where F_i is the increment in the global force matrix on the current step, and R_i is the increment in the global reaction matrix on the previous iteration. As the estimate of the displacement increment matrix on each load step is observed to decrease on each iteration, the matrix Δf_i will be seen to tend toward a null matrix.

The initial approximate solution, Δq^0, is substituted into equation (27) to obtain an improved estimate of the exact solution, and this process is repeated recursively until the error is deemed to be acceptably small, i.e.,

$$\Delta w^m = \Delta w^0 + \sum_{i=1}^{m} \Delta \Delta w^i \tag{29}$$

where m is the iteration number.

From equation (26) it should be clear that when the correct values for the nodal displacement increments, Δq_i^m , are substituted into equation (26), then $f(\Delta q_i^m) \cong 0$. On the other hand, when this is not the case, then equation (26) results in a nonzero value of $f(\Delta q_i^m)$.

The iterative process is terminated when the following condition is satisfied:

$$\frac{\left\| \Delta w^{m+1} \right\|}{\left\| \Delta w^m \right\|} \leq e_{AL} \tag{30}$$

where the double vertical lines signify the Euclidean norm, and e_{AL} is a preset value of allowable error. The total displacement field is subsequently evaluated as follows:

$$w\big(x(t+\Delta t)\big) = w\big(x(t)\big) + \Delta w(x)^{m+1} \tag{31}$$

The above procedure is now validated by using it to solve certain example problems.

F. Validation Problems for the Nonlinear Case

Example Problem #5

Given: A double-cantilevered beam is subjected to a distributed loading, where E=2.06x10^{11} N/m^2, I_{yy}=8.99x10^{-6} m^4, A=0.0145 m^2, l=12.0 m, $\alpha = 1.05x10^{-5}/°C$ and $\Delta T = 50\,°C$.

In addition, the lateral coefficient of friction parameters used to fit the date in Fig. 13 are $k_z^0 = 1.16x10^6\, N/m^2$, $k_z^1 = 6.5x10^5\, N/m^2$, $w_0 = 0.005\, m$ and n=0.05.

Required: a) Obtain an analytic solution for $w = w(x, p_z^0, E, I_{yy})$.

b) obtain a solution using finite elements and compare the two

Solution: a) The solution solves the following differential equation:

$$EI_{yy}\frac{\partial^4 w}{\partial x^4} + P\frac{\partial^2 w}{\partial x^2} + k_z w = p_z \tag{E5.1}$$

Suppose that we choose the following:

$$w(x) = C_1\left[x^2 - \frac{2x^3}{l} + \frac{x^4}{l^2}\right] \qquad 0 \le x \le l \tag{E5.2}$$

where l is the length of the beam and C_1 is a loading constant. It can be seen that the above assumed solution satisfies the following boundary conditions:

$$\begin{aligned} &w(x=0,l) = 0 \\ &\frac{dw}{dx}(x=0,l) = 0 \end{aligned} \tag{E5.3}$$

In order to obtain the forcing function, p_z, equation (E5.2) is now substituted into equation (E5.1) and it is solved, thereby resulting in the following:

$$\begin{aligned} p_z(x) &= C_1 EI_{yy}\frac{d^4}{dx^4}\left[x^2 - \frac{2x^3}{l} + \frac{x^4}{l^2}\right] + C_1 P\frac{d^2}{dx^2}\left[x^2 - \frac{2x^3}{l} + \frac{x^4}{l^2}\right] + C_1\left[k_z^0 - k_z^1\left[\frac{C_1\left(x^2 - \frac{2x^3}{l} + \frac{x^4}{l^2}\right)}{w_0}\right]^n\right]\left[x^2 - \frac{2x^3}{l} + \frac{x^4}{l^2}\right] \\ &= \frac{24C_1 EI_{yy}}{l^2} + C_1 P\left(2 - \frac{12x}{l} + \frac{12x^2}{l^2}\right) + C_1\left[k_z^0 - k_z^1\left[\frac{C_1\left(x^2 - \frac{2x^3}{l} + \frac{x^4}{l^2}\right)}{w_0}\right]^n\right]\left[x^2 - \frac{2x^3}{l} + \frac{x^4}{l^2}\right] \end{aligned} \tag{E5.4}$$

The above forcing function will produce the displacement field given in equation (E5.2).

The next step is to compare the computational results obtained with the finite element algorithm to the exact solution represented by equations (E5.2) and (E5.4). Toward this end, an

allowable error of $e_{AL} = 5.0X10^{-6}$ has been utilized. Fig. 14 shows the predicted vs. exact results for three different finite element meshes. On the basis of these results it is concluded that a 20 element mesh is accurate to five significant digits for the purpose of approximating the displacement field within a rail structure modeled by equations (4)-(8). Furthermore, Fig. 15 shows the finite element predictions using the 20 element mesh on each iteration. On the basis of this, it is concluded that only a few iterations are necessary to accurately predict the effects of nonlinearity in the friction between the ballast-crosstie interface.

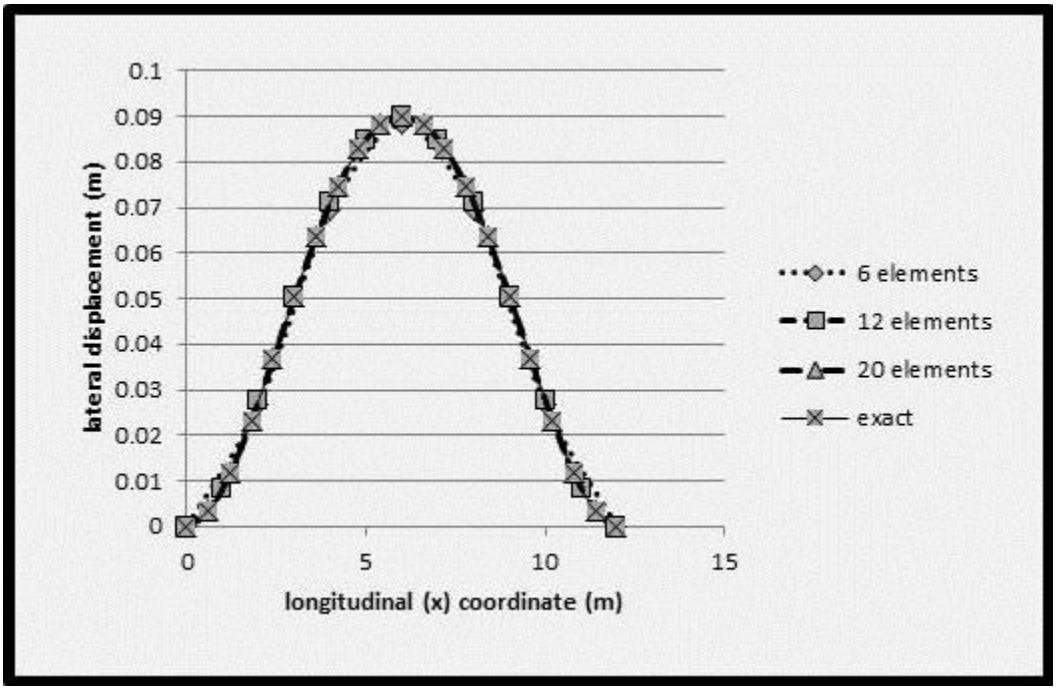

Fig. 14 Comparison of Finite Element Approximations for Three Different Meshes to Exact Solution for Example Problem #5

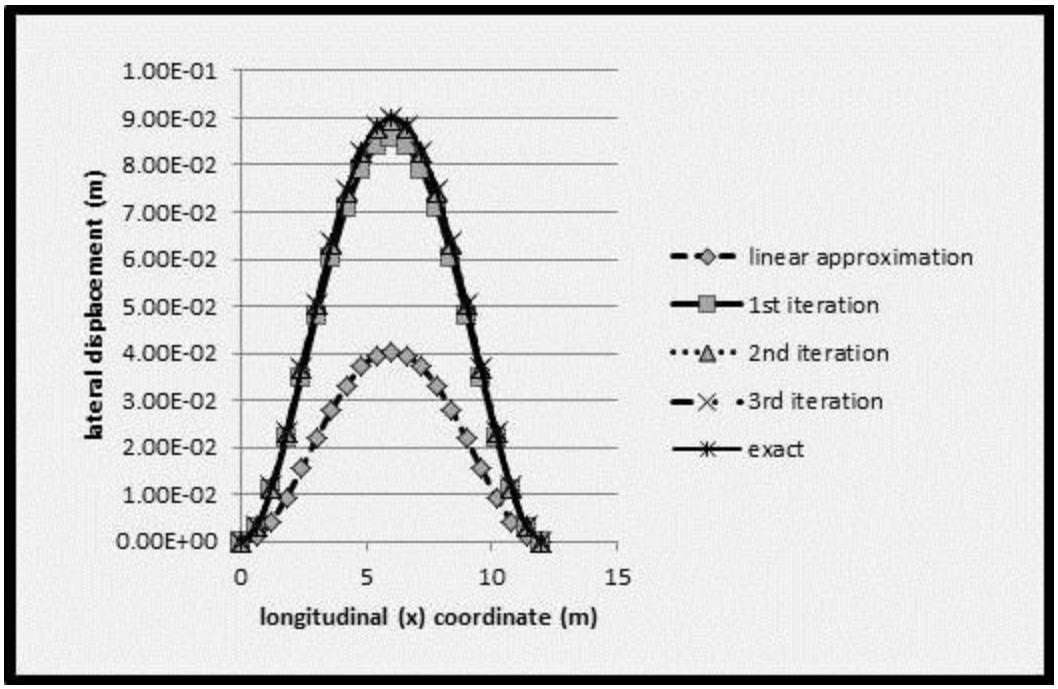

Fig. 15 Comparison of Finite Element Approximations for Each Iteration (20 element mesh) to Exact Solution for Example Problem #5

Conclusion

Herein a formulation has been presented for the purpose of modeling mechanical and thermal load induced buckling in rail structures resting on ballast with nonlinear coefficients of friction, and this formulation has been caste into a nonlinear finite element formulation. The formulation has been validated against both linear and nonlinear example problems with closed-form solutions, and it has been shown that the formulation presented herein is both efficient and accurate when compared to exact solutions.

Unfortunately, exact solutions do not exist for the vast majority of realistic circumstances involving rail structures, and this comprises the primary reason for producing he computational model developed herein. It is envisioned that this model may be utilized in future by railway engineers to assess the necessity for interventions or replacement of sections of track structure for the purpose of avoiding costly and sometimes life-threatening track buckles. The implementation of such a tool will be the purpose of a future paper.

Acknowledgment

The authors are grateful for the funding provided for this research by the UTCRS under USDoT contract no. 602771-00013

References

D Allen and W Haisler (1985) Introduction to aerospace structural analysis, Wiley

D Allen (2013) Introduction to the mechanics of deformable solids: bars and beams, Springer

D Allen, G Fry and D Davis,

L Euler (1744) Method inveniendi lineas curvas, Opera Omni, St. Petersburg, Russia

G Galileo (1637) Dialogues concerning two new sciences, Dover

G Grissom and A Kerr (2006) Analysis of lateral track buckling using new frame-type equations, Int J Mech Sci, 48:21-32

A Kerr (1974) The stress and stability analyses of railroad tracks, J Appl Mech, 41:841-848

A Kerr (1978) Analysis of thermal track buckling in the lateral plane, Acta Mechanica, 30:17-50

N Lim, N Park and Y Kang (2003) Stability of continuous welded track, Computers & Structures, 81:2219-2236

D Little, D Allen and A Bhasin (2016) Modeling and Design of Flexible Pavements and Materials, Springer

J Oden and E Ripperger (1981) Mechanics of elastic structures, Second Edition, McGraw-Hill

Railroad Accident Statistics (2015) Federal Railroad Administration, downloaded at:http://safetydata.fra.dot.gov/officeofsafety/publicsite/Query/TrainAccidentsFYCYWithRates.aspx

D Read, R Thompson, D Clark and E Gehringer (2011) Results of Union Pacific concrete tie track panel shift tests, Technology Digest, TD-11-004

J Reddy (1984) An Introduction to the Finite element Method, McGraw-Hill

S Timoshenko (1915) Strength of rails, Transactions of the Institute of Ways and Communications, St. Petersburg, Russia

S Timoshenko (1927) Method of analysis of statical and dynamical stresses in rail, Proc. Second International Congress for Applied Mechanics, Zurich

V Tvergaard and A Needleman (1981) On localized thermal track buckling, Int J Mech Sci, 23:577-587